UNIVERSITY OF WEST BOHEMIA

Applied and Computational Mechanics 3 (2009) 375–390

Applied and Computational Mechanics

A refined description of the crack tip stress field in wedge-splitting specimens – a two-parameter fracture mechanics approach

S. Seitl[a,*], Z. Knésl[a], V. Veselý[b], L. Řoutil[b]

[a] *Institute of Physics of Materials, Academy of Sciences of the Czech Republic, v.v.i. Žižkova 22, 616 62 Brno, Czech Republic*

[b] *Institute of Structural Mechanics, Faculty of Civil Engineering, Brno University of Technology, Veveří 331/95, 602 00 Brno, Czech Republic*

Received 24 August 2009; received in revised form 6 November 2009

Abstract

The paper is focused on a detailed numerical analysis of the stress field in specimens used for the wedge splitting test (WST) which is an alternative to the classical fracture tests (bending, tensile) within the fracture mechanics of quasi-brittle building materials, particularly cementitious composites. The near-crack-tip stress field in the WST specimen is described by means of constraint-based two-parameter fracture mechanics in the paper. Different levels of constraint in the vicinity of the crack tip during fracture process through the specimen ligament are characterized by means of the T-stress. Two basic shapes of WST specimen – the cube-shaped and the cylinder-shaped one – are investigated and the determined near-crack-tip stress field parameters are compared to those of compact tension (CT) specimens according to the ASTM standard for classical and round geometry. Particular attention is paid to the effect of the compressive component of the loading force (complementing the splitting force) acting on the loaded side of the specimen and its reaction from the opposite part of the specimen on the stress field in the cracked body. Several variants of boundary conditions on the bottom side of the specimen used for this kind of testing procedure are also considered. The problem is solved numerically by means of the finite element method and results are compared with data taken from the literature.

Keywords: wedge splitting test, crack tip stress field, two-parameter fracture mechanics, fracture parameters, numerical simulation

1. Introduction

For determination of the fracture-mechanical parameters of quasi-brittle materials used commonly in the building industry, particularly cement-based composites such as concretes and mortars, specific experimental tests on notched specimens under bending (e.g. three- or four-point bending of notched beams or cylinders), tension (e.g. single or double edge notched or dog-bone specimens) or eccentric compression (e.g. double edge notched cubes or prisms and round notched cylinders) are usually performed [5, 15, 34, 39].

However, the influence of the bended specimen's own weight at the performed test's record is significant and cannot be ignored, especially in the case of materials with low tensile strength, e.g. early-aged concretes and mortars [28]. Moreover, a substantial portion of the testing specimen's volume remains elastic and does not directly participate in the failure test, which causes an unnecessary increase in the material required for preparation of the testing specimen. There is either a superfluous amount of the fresh concrete/mortar necessary for the casting of the

*Corresponding author. Tel.: +420 532 290 348, e-mail: seitl@ipm.cz..

testing specimens in the case of those specimens prepared simultaneously with the structure's realisation or an immoderate demand for the volume of material necessary to be taken from already existing structures.

The performance of the tensile tests is, on the other hand, very demanding on the experimental equipment, which encounters e.g. the need for high stiffness of the testing machine and fittings (e.g. [5, 40, 44]) as well as the necessity of a sophisticated apparatus controlling the loading rate through feed-back signal from gauges measuring displacements or crack opening displacements (e.g. [1]).

Eccentric compression is disadvantageous, especially for the reason that also applies to some cases of both above-mentioned loading configurations; scilicet, a substantial amount of elastic energy stored in the specimen and the testing machine (frame, fittings) is released suddenly at the start of the crack/notch propagation, which causes an instable fracture [41].

A convenient alternative to the bending or tensile tests is presented by a wedge splitting test (WST) proposed by [24] and later developed in [7] and other works. The WST is an adaptation of the common compact tension (CT) test which eliminates the disadvantages stemming from the usually insufficient toughness of the fittings between the CT specimen and the testing machine (cumulating of elastic energy resulting in lower test stability). A compressive load induced by the loading device is transformed into a tensile loading opening the initial notch via special testing arrangement based on the wedge mechanism (see fig. 1a. An ordinary electromechanical testing machine with a constant actuator displacement rate can be used and no sophisticated test stability control apparatus (i.e. closed loop control unit with e.g. crack tip opening displacement as a feedback signal) is necessary. A cardinal advantage of this arrangement is its very high stiffness in comparison to the loading chain of the common CT test or other, especially tensile, tests.

As is obvious from fig. 1, the test specimens can be prepared either from standard cube, beam or cylinder-shaped specimens cast into standard moulds, or as prismatic or cylindrical specimens taken from existing structures by sawing or core-drilling, respectively. The WST is extensively used for various experimental studies and recently an increase in usage of the testing method has been registered (e.g. [9, 14, 19, 25, 28, 38, 46, 47, 48]).

The determination of fracture-mechanical properties of materials from records of fracture tests is conditioned by a proper fracture-mechanical description of the test in question. In the case of common testing geometries relevant information can be found summarized in the classical works in the field of fracture mechanics (e.g. [2, 5, 15, 29, 34]), handbooks ([26, 36]) or other works [20]. Fracture parameters for the WST are not so widely reported. Stress intensity factors (SIF, K-factor) for particular variants of the WST (cube-shaped specimens) can be found in literature, e.g. [10, 30]. However, they are utilizable within a classical (single-parameter) fracture mechanics approach only, which is inaccurate (insufficient) for application in the case of quasi-brittle fracture. Approximate expressions of the terms of Williams' series [45] approximating the stress field in the cracked body up to the order of 5 for particular dimensions of cube-shaped WST specimens were introduced for the first three coefficients in [18] and further developed for five coefficients in [16]. These results cover a considerably wide range of exploitable dimensions of cube-shaped WST specimens with two types of boundary conditions in the area of application of the load to the specimen by the wedge mechanism. However, they are valid only for a limited range of variants of support configuration on the bottom side of the specimen.

In this paper, the numerical analysis of stress field for wedge splitting geometry in the framework of two-parameter fracture mechanics is introduced. The stress intensity factor K and the T-stress for cube- and cylinder-shaped WST specimens are determined and they are compared

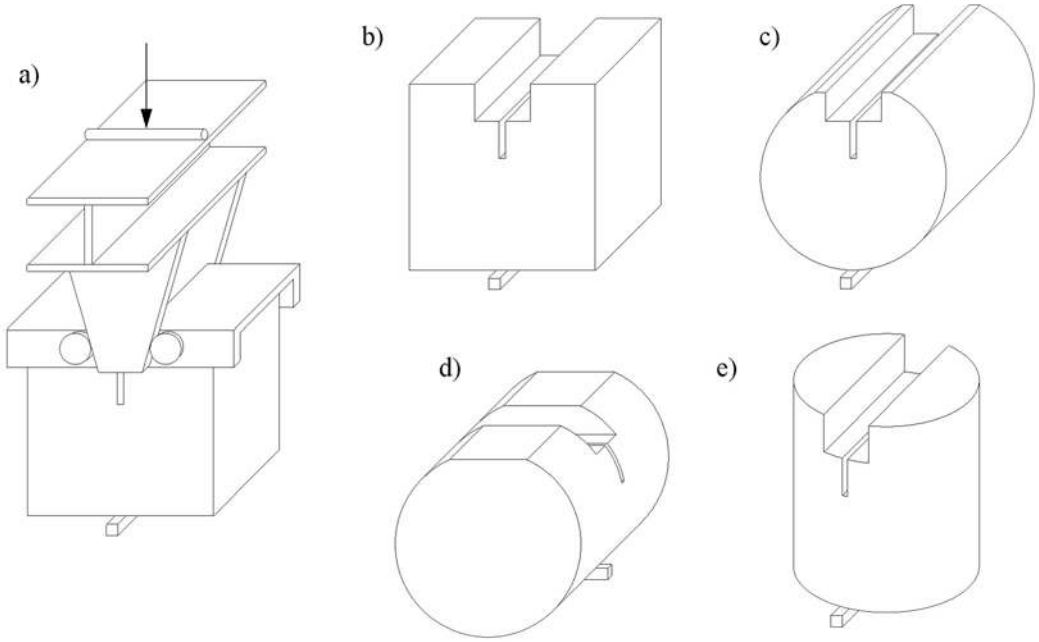

Fig. 1. Wedge splitting test geometry: sketch of stiff fixtures transferring the load from the testing machine to the specimen (a), several variants of specimen shapes applicable for WST prepared from standard cube (b) and cast or core-drilled cylinder (c, d, e) (inspired by [24])

to results corresponding to the similar testing configuration – the classical and round CT specimens. The effects of different boundary conditions on both the loaded and the supported side of the WST specimen on the calculated fracture parameters are examined. The influence of friction of the roller bearing on the values of fracture parameters (K, T-stress) is briefly discussed. The present paper follows on from and elaborates the previous studies of the authors on this subject [31, 32, 33].

This paper is divided into several sections. After this introduction the motivation of the work is clarified with particular definition of the objectives of the analyses performed. Next, the theoretical background as a basis for the calculations conducted is briefly explained. A section devoted to modelling details is then followed by analysis and discussion of the results. The importance of the research introduced with substantial conclusions is stated in the last section.

2. Motivation, analysis objective definition

Knowledge of the stress field in the cracked specimen, or at least its accurate enough estimation, provides the possibility of constructing the size and shape of the fracture process zone (FPZ) characteristic for the fracture of quasi-brittle cementitious composites, as is proposed by [42, 43]. This method is based on multi-parameter linear elastic fracture mechanics and classical non-linear models for quasi-brittle fracture. A technique of this kind enables the specification of the energy dissipated in the FPZ evolving at the macroscopic crack tip during fracture process in quasi-brittle materials to its volume, which might contribute to a more precise determination of the fracture-mechanical parameters of quasi-brittle materials. The numerical analysis proposed in the paper has been motivated particularly by this issue.

The numerical study consists of three parts which are described in following sections in detail.

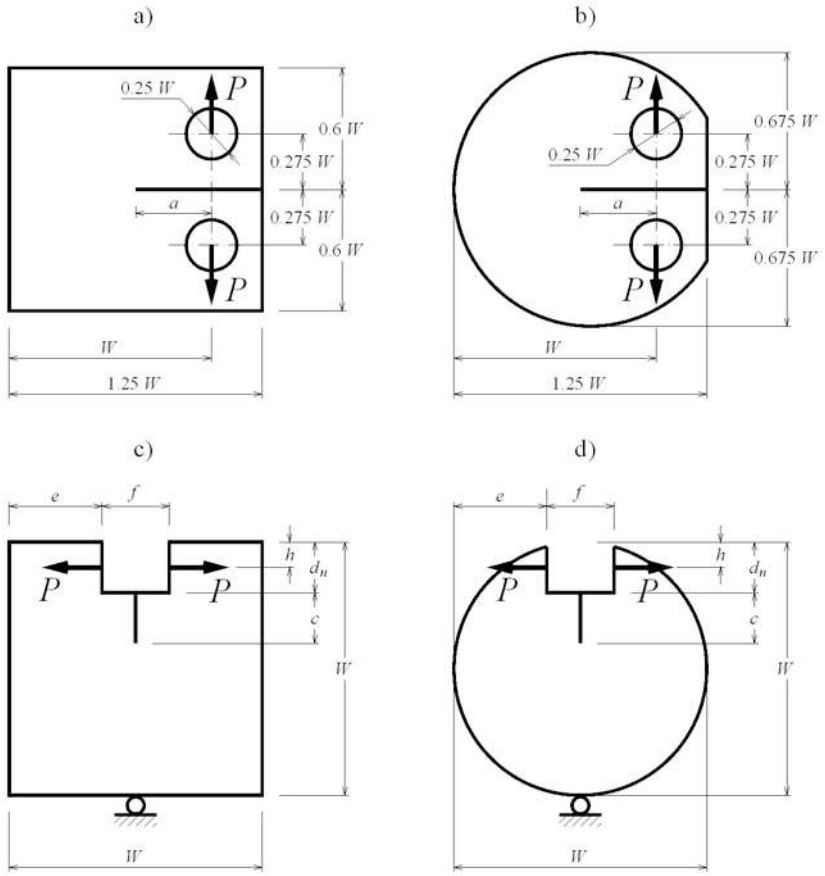

Fig. 2. The geometry of the compact tension test with classical (CT – a) and round (RCT – b) compact tension specimen; the geometry of wedge-splitting test with cube-shaped (c) and cylinder-shaped (d) specimens

2.1. Study I

In this study the characteristics of the near-crack-tip stress field in the cube- and cylinder-shaped WST specimen (figs. 2c and 2d, respectively) are compared to those of the classical and round CT specimen (figs. 2a and 2b, respectively) that are usual (standard) testing specimens in the case of fracture testing of metals [4]. The CT geometry was chosen due to its similarity to the WST geometry from both the specimen's shape and the imposed load point of view. In this study the loading of the WST specimens was considered in a simplified way – the splitting component of the loading force[1] was only assumed.

For numerical calculations of both geometries the value $W = 100$ mm was used. Other dimensions of the WST geometries were equal to $e = 35$ mm, $f = 30$ mm, $h = 10$ mm, $d_n = 20$ mm (the dimensions are indicated in fig. 2). The initiation notch of length a and c for CT and WST geometry, respectively, was modelled as a crack where their values varied so that parameter α indicating the relative crack length lies in the interval $\langle 0.2, 0.8 \rangle$. In the present numerical study the relative crack length α is defined as a ratio of the effective crack length, i.e. the distance from the point of the force application to the crack tip, and the effective specimen

[1]The loading force introduced by the testing machine is decomposed through the wedge into the splitting and the compressive component. As the angle of the wedge ranges usually from $10°$ to $15°$, the value of the compressive component in relation to the splitting on is very low.

width, i.e. the distance from the point of the force application to the end of the specimen:

$$\alpha = \frac{a}{W} \tag{1}$$

for CT and RCT specimens, see figs. 2a and 2b, and

$$\alpha = \frac{c + (d_n - h)}{W - h} \tag{2}$$

for cube- and cylinder-shaped WST specimens, see figs. 2c and 2d.

2.2. Study II

Investigation of the stress field in the WST specimens has followed the specification of the boundary conditions in the area of introducing of the load – the component of the loading force inducing the compression of the specimen was taken into account. Both expected components of the loading force in the case of WST specimen are shown in fig. 3. The applied splitting force P_{sp} (acting horizontally in the figure) is related to the compressive load P_v (vertical), see e.g. [30, 35], as:

$$P_{\mathrm{v}} = \frac{1}{2} P_{\mathrm{sp}} k, \tag{3}$$

where

$$k = \frac{2 \tan \alpha_{\mathrm{w}} + \mu_{\mathrm{c}}}{1 - \mu_{\mathrm{c}} \tan \alpha_{\mathrm{w}}}. \tag{4}$$

Symbol α_{w} represents an angle of the wedge and μ_{c} refers to friction in the roller bearings. A single support on the axis of symmetry presents the only boundary condition on the specimen back-face (see fig. 3).

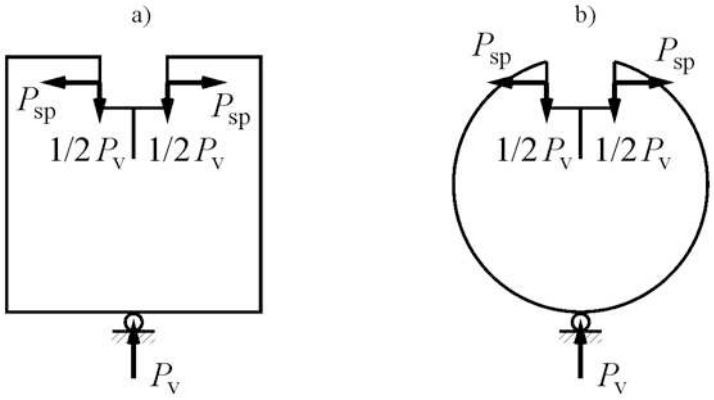

Fig. 3. The cube- and cylinder-shaped WST specimens – an indication of the loading determined by the boundary conditions

The influence of the friction in roller bearings which transfer the load from the wedge to the specimen was also investigated. The coefficient of friction μ_{c} usually varies between 0.001 and 0.005 for bearings used within the experimental setup, see e.g. [13]. In our case two values of coefficient μ_{c} are used as the lower and upper bound to cover all possible values of the friction coefficient. The first one was set to 0; it means that there is no friction in the bearings, and second one to 0.005, which represents the maximal friction in the roller bearings. The dimensions of the WST specimens were considered the same as in the previous study.

2.3. Study III

The next study was focused particularly on the cube-shaped WST specimens. Precise representation of the loading (both components of the loading force) was taken into consideration and the influence of the boundary conditions on the bottom side of the specimen was chiefly investigated.

The study supplements the work by Karihaloo et al. [16] in this aspect. In figs. 4a and 4b schemes of testing configuration analysed in [16] are depicted. Schemes in figs. 4c up to 4e represent variants of boundary conditions on which own computations were conducted. On the other hand, only the values of the stress intensity factor K and the T-stress along the crack propagation through the specimen ligament were computed in contrast to first 5 terms of the Williams series presented in [16], as is noted above. Another improvement covered by the proposed paper in comparison to the results published in [16] is the investigation of the influence of the vertical component of the loading force on the values of the near-crack-tip stress state parameters (compare figs. 4a with 4c or 4b with 4e, respectively). This issue is partly also the subject of the study described in the previous section. The specimen dimensions correspond to the previous studies and are indicated in fig. 4.

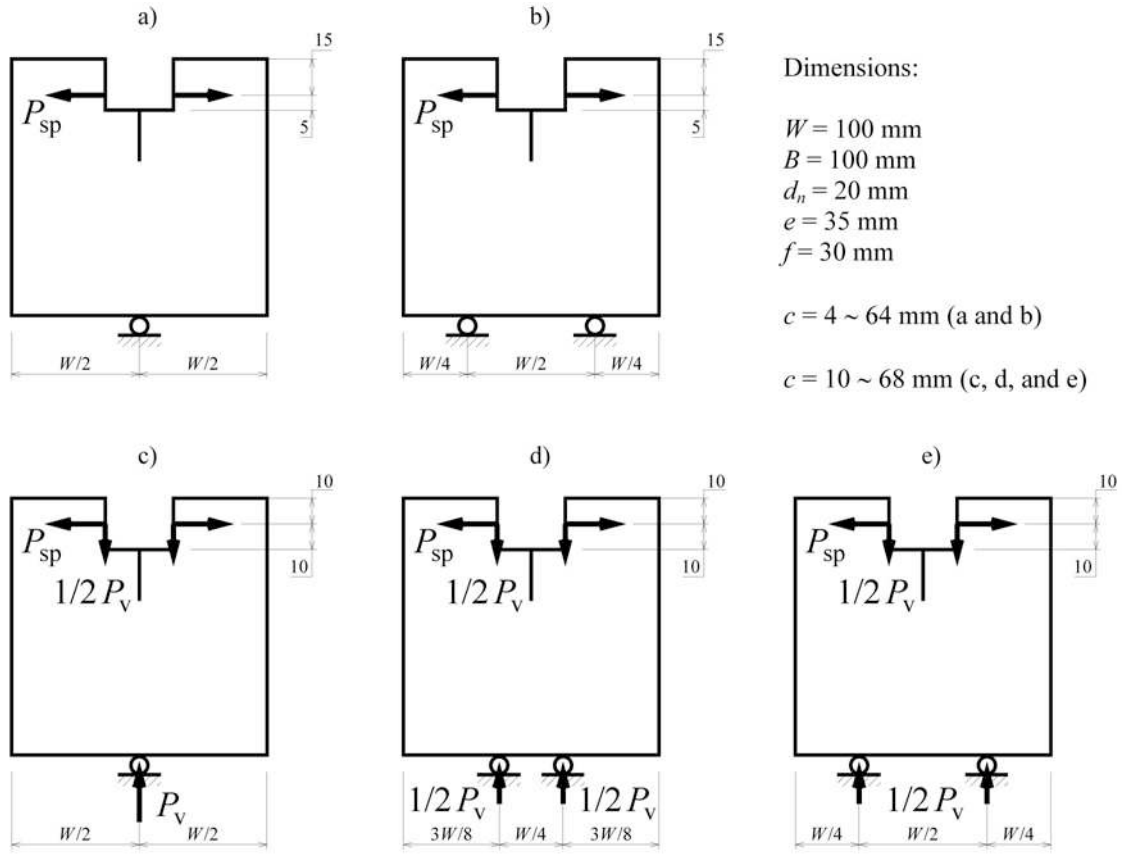

Fig. 4. Considered specimen dimensions, components of loading force and variants of supports: (a and b) Karihaloo et al. [16], (c, d, and e) own computations

3. Theoretical background

According to two-parameter fracture mechanics approach which uses T-stress as a constraint parameter, the stress field around the crack-tip of a two-dimensional crack embedded in an isotropic linear elastic material subjected to normal mode I loading conditions is given by the following expressions [45, 2]:

$$\begin{aligned} \sigma_{xx} &= \frac{K_I}{\sqrt{2\pi r}} \cos\left(\frac{\theta}{2}\right)\left[1-\sin\left(\frac{\theta}{2}\right)\sin\left(\frac{3\theta}{2}\right)\right]+T \\ \sigma_{yy} &= \frac{K_I}{\sqrt{2\pi r}} \cos\left(\frac{\theta}{2}\right)\left[1+\sin\left(\frac{\theta}{2}\right)\sin\left(\frac{3\theta}{2}\right)\right] \\ \tau_{xy} &= \frac{K_I}{\sqrt{2\pi r}} \cos\left(\frac{\theta}{2}\right)\sin\left(\frac{\theta}{2}\right)\cos\left(\frac{3\theta}{2}\right) \end{aligned} \tag{5}$$

where r and θ are the polar coordinates and x and y are the Cartesian coordinates, both with origins at the crack tip. K_I is the stress intensity factors (SIF) for mode I, σ and τ are the normal and shear stress, respectively. The T term in the first line of equation (6) is the elastic T-stress which is the second constant term corresponding to a uniform parallel stress $\sigma_{xx} = T$. Thus, in two-parameter based fracture mechanics, the stress field is expressed by means of the two parameters, the stress intensity factor K_I and the T-stress (see e.g. [20, 27]).

The SIF and the T-stress according to [23] may be normalized expressed by stress biaxiality ratio B as follows:

$$B_1 = \frac{K_I}{K_0}, \qquad \text{where} \qquad K_0 = \frac{P_{sp}}{t\sqrt{W}} \tag{6}$$

and

$$B_2 = \frac{T\sqrt{\pi a}}{K_I}, \tag{7}$$

where P_{sp} is the horizontal splitting loading force, t is the thickness, W is the fundamental dimension (specimen width) and a represents the crack length. In the present numerical study the crack length a is defined as a distance from the point of the force application to the crack tip, see section 2.1.

4. Modelling

The material input data for the concrete used in the numerical simulation are chosen as follows: Young modulus $E = 44\,000$ MPa and Poisson's ratio $\nu = 0.2$.

The stress intensity factor K and the T-stress values were computed by means of the finite element method either using direct techniques [49] or quarter-point crack-tip elements for their determination ([37, 11]). Generally, the direct methods need extreme mesh refinement close to the crack tip in comparison with the method employing quarter-point elements. For direct method the estimation of the fracture parameters is derived directly from the singular stress description, see eq. (5).

As a first step, the 2D finite element method solution is employed to the CT and RCT specimens to verify the accuracy of used numerical model. Subsequently the above-mentioned methods are applied to fracture parameters calculations for both shapes of WST specimens. The commercial finite element program ANSYS is used to analyze all the models presented here.

Note that the geometries are symmetric including both the specimen shapes and the loading conditions; therefore only one half of each specimen was modelled. Different finite element

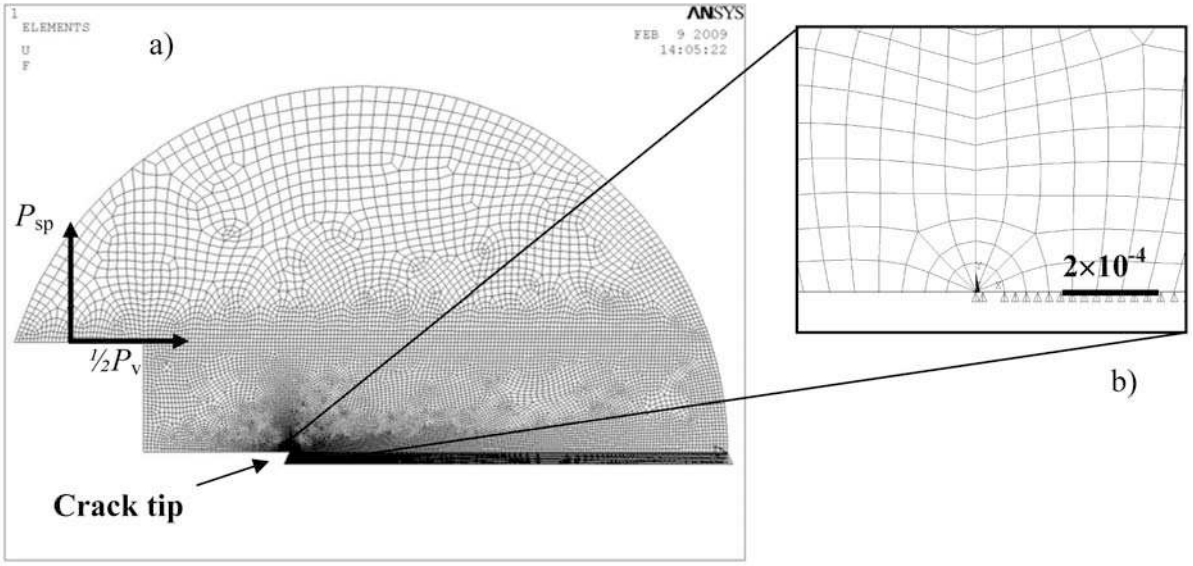

Fig. 5. The finite element mesh used in the simulations: a) One half of the cylinder shaped WST specimen used for FEM calculation, b) detailed view of the small region near the crack tip (a quarter-point crack-tip element was used)

models are constructed for each of the a/W ratios investigated. A typical finite element mesh used in the computations is shown in fig. 5 together with a detailed view of the small region near the crack tip. The size of the smallest element in the crack tip is 5×10^{-5} mm.

5. Results and discussion

The results obtained from the numerical study are divided into following three subsections correspondingly to section 2.

5.1. Study I

Numerical results comparing the normalized values of the SIF (i.e. B_1) and T-stress (i.e. B_2) for the cube- and cylinder-shaped WST specimens (see figs. 2c and 2d, respectively) with those of the classical and round CT specimens (see figs. 2a and 2b, respectively) are plotted in fig. 6. The values of the B_1 and B_2 for the classical and round CT specimens can be found in literature, see e.g. [20].

The compact tension geometry from the ASTM standard [4] is similar, in some geometrical aspects; to the wedge splitting geometry and it is possible to expect similar values of the normalized stress intensity factor B_1 related to SIF by eq. (6). The dependences of normalized stress intensity factor B_1 as a function of α for four considered test geometries are presented in fig. 6 left. The graph shows that the normalized SIF values are similar for corresponding specimen shapes of wedge splitting and compact tension geometry (cubic-shaped WST and CT, cylindrical WST and RCT). This fact is obvious especially for long cracks ($\alpha > 0.5$), where the influence of the loading setup to the stress state within the specimen can be supposed to vanish.

The normalized T-stress values B_2 defined as a function T-stress in eq. (6), are plotted in fig. 6 right. According to the results obtained, it can be seen that the $B_2(\alpha)$ functions for the WST geometry vary from negative to positive values for both specimen shapes. This is contrary to the compact tension specimen (CT and RCT), where the B_2 values are positive for each α.

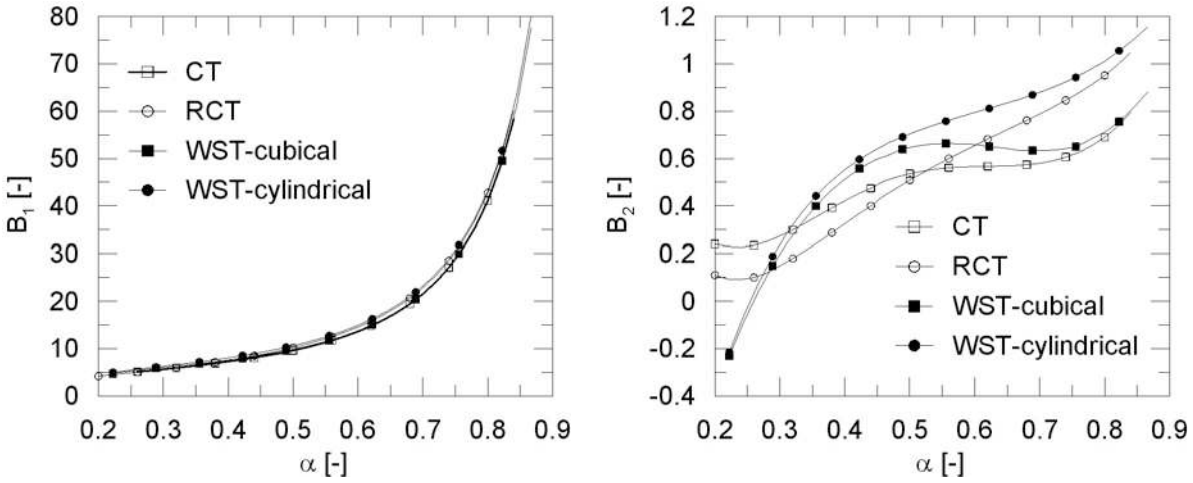

Fig. 6. Normalized values of the stress intensity factor K, B_1 (left), and T-stress, B_2 (right), for four considered specimen shapes

5.2. Study II

Numerical results of this study show the influence of the compressive load P_v (vertical) defined in eq. (4), see fig. 3. As the second step in this section the influence of the friction in roller bearings which transfer the load from the wedge to the specimen was investigated.

The numerically calculated values of the normalized SIF (i.e. B_1) and T-stress (i.e. B_2) for cube- and cylinder-shaped WST specimens are given in fig. 7 (left) and 7 (right) and fig. 8 (left) and 8 (right), respectively. In these figures there are always three curves plotted: *i)* marked as WST – the curve for cube-/cylinder-shaped WST loaded only by splitting force, *ii)* WST_P – cube-/cylinder-shaped WST loaded by both components of the loading force, i.e. the splitting force P_{sp} and the vertical compressive force P_v, without considering friction in roller bearings (i.e. $\mu_c = 0$), and *iii)* WST_P_μ – the same as in *ii)* with considering the maximal potential value of friction coefficient ($\mu_c = 0.005$).

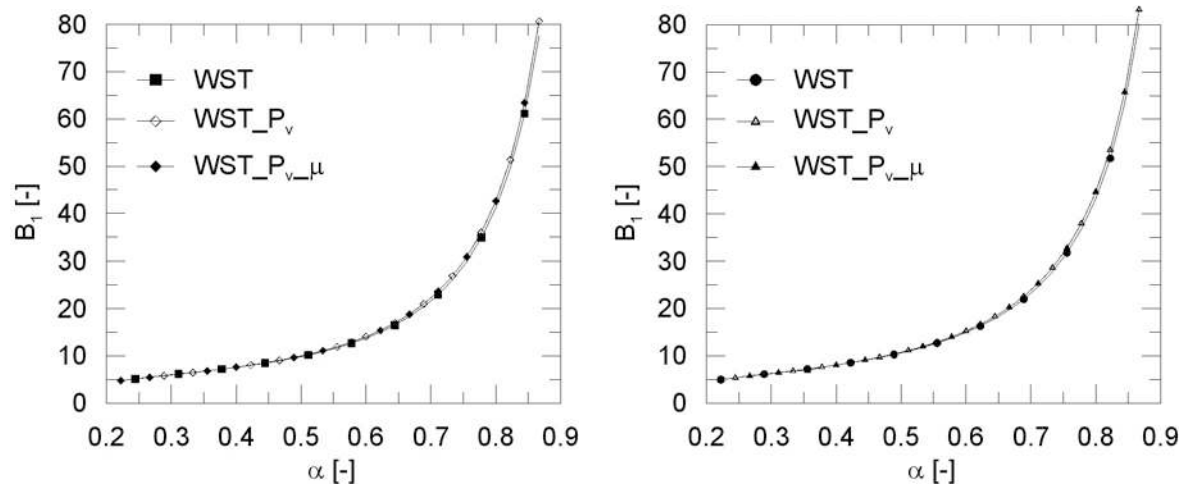

Fig. 7. Normalized values of the stress intensity factor K, B_1, for cube-shaped (left) and cylinder-shaped (right) WST specimen

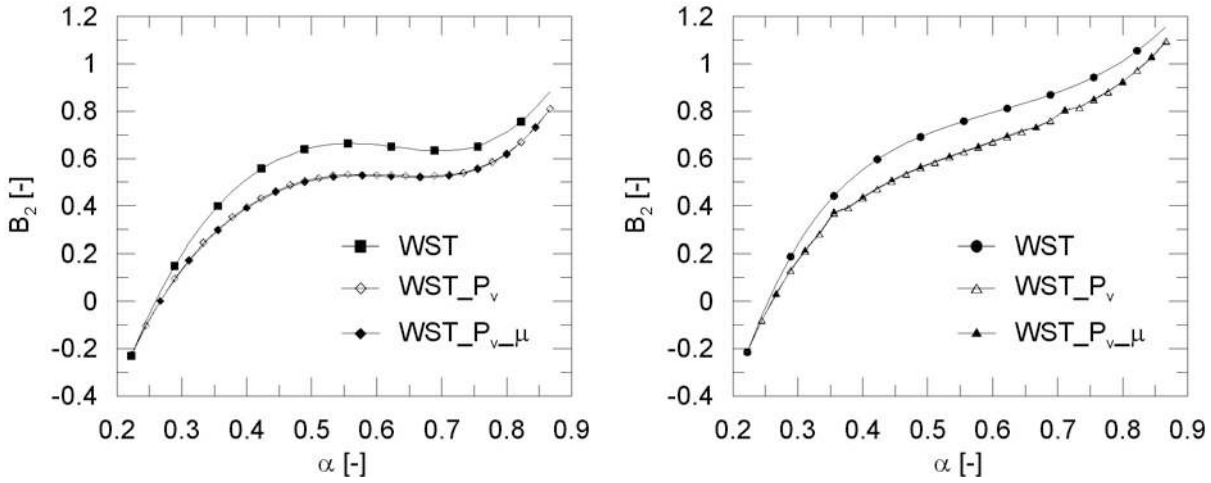

Fig. 8. Normalized values of the T-stress, B_2, for cube-shaped (left) and cylinder-shaped (right) WST specimen

The results for cube-shaped WST specimen are shown in fig. 7 and 8 on the left. The B_1 as a function of α have the same trend for all (WST, WST_P and WST_P_μ) curves, see fig. 7 left. A slight difference of the B_1 values (weak increase) can be seen for analyses considering the vertical compressive force in comparison to the analysis neglecting the effect of the bottom support, however, only for $\alpha > 0.7$. The influence of the bottom support (differences between the WST and WST_P curves) is more pronounced than the influence of the friction in the roller bearings (differences between WST_P and WST_P_μ curves).

The normalized values of second parameter – T-stress, expressed by B_2, as a function of α are presented in fig. 8. The influence of the vertical compressive load (WST_P) plays a dominant role on the parameter B_2 (see differences between WST and WST_P curve), the influence from the friction in roller bearings is insignificant. The WST_P and WST_P_μ curves are similar and the error introduced by neglecting the friction in bearings (even at its maximal value) is less than 2 %, which is in agreement with recommendations from the literature [30, 35].

The results for the cylinder-shaped WST specimen are shown in fig. 7 and 8 on the right. The graphs shows that the normalized stress intensity factor values B_1 are similar for all three studied cases of wedge splitting test, similarly to the cube-shaped WST. This fact is especially obvious for short cracks ($\alpha < 0.6$), where the influence of the loading set-up to the stress state within the specimen can be regarded as negligible.

The normalized T-stress, i.e. $B_2(\alpha)$ functions, vary from negative to positive values for all loading cases. The influence of the vertical compressive load plays a dominant role in the parameter B_2, as in the case of the cube-shaped WST, the change due to the friction in roller bearings is also insignificant.

5.3. Study III

The final study focused on the cube-shaped WST specimen and covered the influence of alternative supports, see figs. 4c (WST_P$_v$), 4d (WST_P$_v$_1/4), 4e (WST_P$_v$_1/8). The numerically calculated values of the normalized stress intensity factor $K(B_1)$ and T-stress (B_2) are given in figs. 9 left and 9 right, respectively.

The normalized SIF values, B_1, are similar for WST cube-shaped specimen without vertical load and three specimens including vertical load with various supports (a single central line

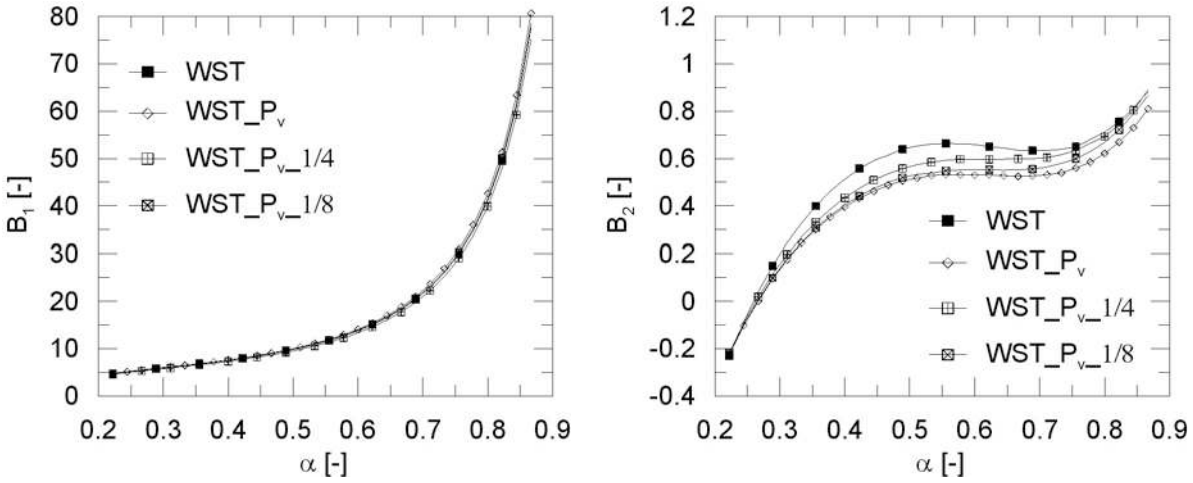

Fig. 9. Normalized values B_1 of the stress intensity factor K_I (left) and normalized values B_2 of the T-stress (right) for considered specimen dimensions and boundary conditions

support and two line support), as shown in the fig. 9 and it is possible to conclude that the influence of various supports on values of SIFs is not significant.

The normalized T-stress values from the conducted FEM analysis, expressed as B_2, are plotted in fig. 9 right. According to the results obtained, it is obvious that the $B_2(\alpha)$ functions for the WST geometry vary from negative values for short cracks to positive values for relative crack lengths larger than approximately 0.25 in all cases studied. The influence of loading arrangements studied on the values of B_2 is significant especially in the interval $\alpha \in (0.3; 0.8)$. Note that the interval is commonly used within the measurement of fracture parameters in the case of the mentioned WST geometry.

6. Comparison with data from literature

As was mentioned in the introduction, Guinea et al. [10] presented solely values of SIF for WST geometry. Karihaloo & Xiao [18] compared those values were with their own results and reported differences was less than 2 %. Therefore, in this article the results given by [18] (elaborated later in [16]) are compared with our presented results. These comparisons for the normalized SIF K_I (B_1) and the T-stress (B_2) are summarized in figs. 10 and 11, respectively.

In the graphs in figs. 10 and 11, there are five curves plotted:, *i)* the curve calculated for WST loaded only by the splitting force P_{sp}, see fig. 2c (marked as WST), *ii)* the curve calculated for WST loaded by both components of the loading force, i.e. the splitting force P_{sp} and the vertical compressive force P_v, see fig. 4c, (WST_P$_v$) *iii)* and *iv)* the curves calculated for WST loaded by both the splitting and the vertical compressive force with two supports with various distances, see fig. 4d (WST_P$_v$_1/4) and fig. 4e (WST_P$_v$_1/8), respectively, and v) the curve constructed from data by Karihaloo et al. [16] corresponding to the configuration depicted in fig. 4a.

It should be noted that in the article [16] the authors did not specify whether the vertical component of the load was considered in the numerical computations or not. Fig. 11 shows good agreement of the WST curve and the Karihaloo et al [16] curve, their geometry and boundary conditions are depicted in fig. 2c (WST) and in fig. 4a (Karihaloo et al. [16]). This indicates that the vertical component of the loading force was not considered in [16].

A high level of crack-tip constraint can reduce fracture toughness and, in the case of fatigue cracks, can reduce fatigue crack growth rate [21]. The knowledge of constraint enables

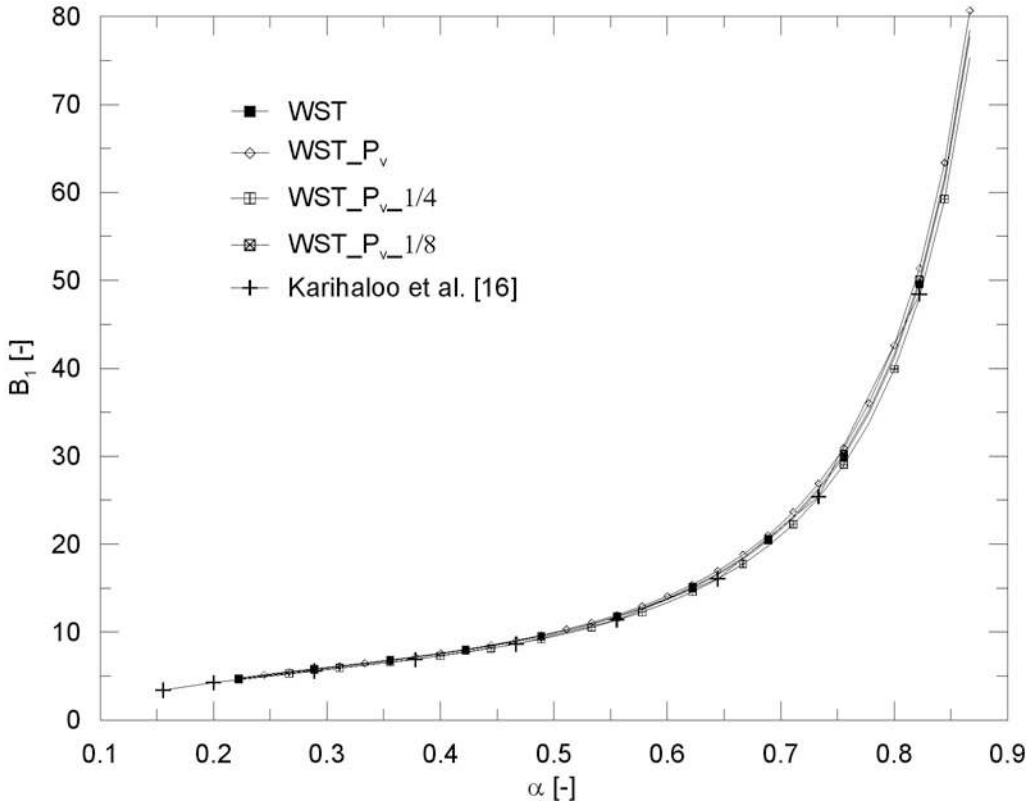

Fig. 10. Normalized values B_1 of the stress intensity factor K_I for considered specimen dimensions and boundary conditions

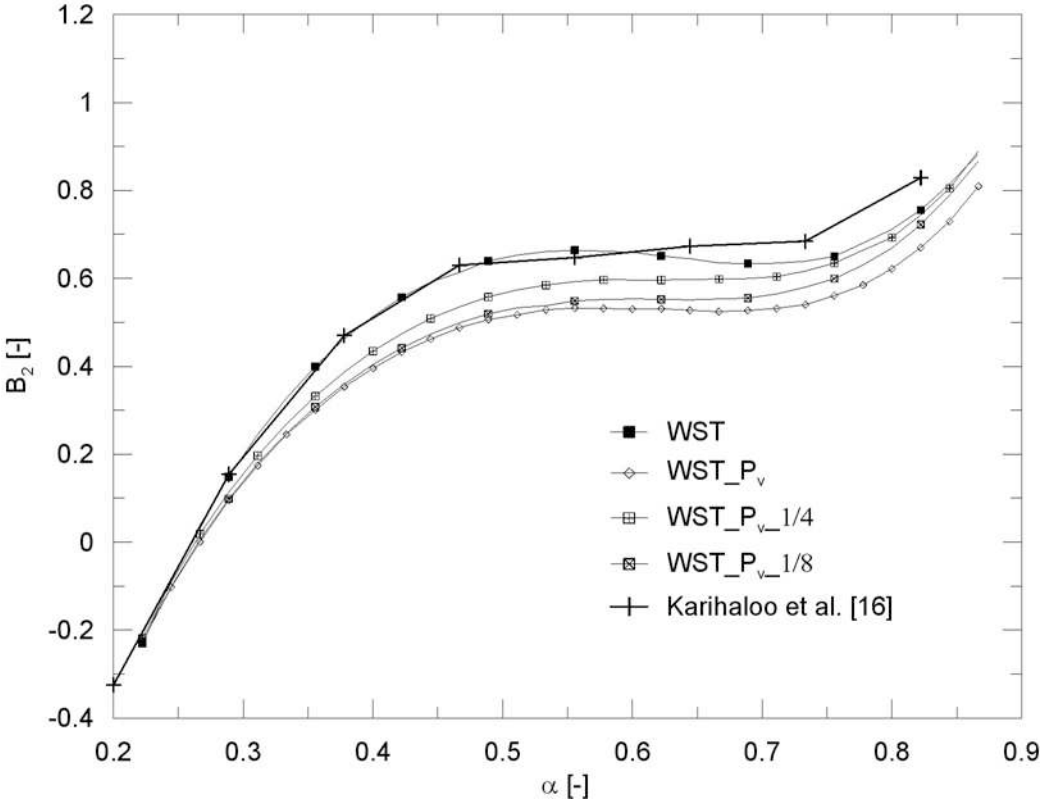

Fig. 11. Normalized values B_2 of the T-stress for considered specimen dimensions and boundary conditions

a transferability of fracture toughness values obtained on laboratory specimens to engineering structures. In general, two-parameter fracture mechanics approaches imply that the laboratory specimens must match the constraint of the structure. The two geometries must have the same B_2 values in order to transfer fracture toughness from laboratory specimens to engineering structures, see e.g. [27]. The approach of two-parameter fracture mechanics is descriptive but not predictive. From this point of view the approximation of B_2 values calculated for homogenous specimens is sufficient and can be used to characterize constraint in cases when heterogeneity not essential as well. In order to use the two parameter fracture mechanics approach in fracture analysis, the constraint for the considered wedge splitting test has to be calculated.

7. Conclusions

A finite element numerical analysis of the near-crack-tip stress fields for several variants of WST specimen shapes (cubical and cylindrical) with various boundary conditions was performed by means of a constraint-based two-parameter fracture mechanics approach. The study consists of three parts each of which was focused on selected aspects:

i. Comparison of the cube- and cylinder-shaped WST specimens with classical CT and round CT specimens.

ii. Consideration of the compressive component of the loading force together with a single central support on the back-face of the specimen; investigation of the influence of friction in the roller bearings.

iii. Consideration of the compressive component of the loading force together with several variants of supports proposed in the literature.

The analysis procedures and results were compared with existing solutions from the literature. The following conclusion may be drawn from the results obtained:

- The stress intensity factors for cube-shaped WST and CT specimens and cylinder-shaped WST and RCT specimens, respectively, are similar. That holds true even for mutual comparison of cube-and cylinder-shaped WST specimens. This fact is especially pronounced for long cracks ($\alpha > 0.5$).

- The T-stress depending upon the crack depth ratio α varies from negative to positive values with increasing α for both WST specimen shapes, contrary to the CT geometry, where the T-stress is always positive.

- The influence of the geometry is much stronger on the values of T-stress than the stress intensity factors.

- The influence of the vertical compressive force, i.e. the reaction from the support at the back-face of the specimen, is much stronger on the values of T-stress than on the K-factors.

- The friction in roller bearings with usual intensity influences the results of the wedge splitting test negligibly.

- Normalized values of K-factor (B_1) are almost the same in the whole range of the relative crack length α for all studied variants of the WST boundary conditions. They are in good agreement with the results published in the literature [10, 16, 18].
- Normalized values of the T-stress (B_2) depend noticeably on both considered groups of changes of boundary conditions, i.e. both in the part of the application of the load (based on considering the compressive force component or not) and on the opposite side of the specimen (one or two supports, different distances of the supports).
- Neglecting of the compressive component of the loading force increases stress constraint at the crack tip. This tends to underestimation of the size of the zone of failure, which consequently causes an overestimation of the values of the determined fracture-mechanical parameters.
- An increase in the distance of the two supports on the bottom side of the specimen leads to an increase in the value of the T-stress.

The present results can be used for more reliable determination of fracture parameters of concrete-like materials. The utilization of the procedure for the FPZ size and shape estimation shows that knowledge of the higher order terms of the crack tip stress field is necessary [42, 43, 33], therefore attempts to compute more than the two members (i.e. K-factor and T-stress) of the Williams' series approximating the stress field in the cracked body are in preparation.

Acknowledgements

The work has been supported by the grant project of the Grant Agency of the Academy of Sciences of the Czech Republic No. KJB200410901 and by the research project of the Czech Science Foundation No. 101/08/1623.

References

[1] Akita, H., Koide, H., Tomon, M., Sohn, D., A practical method for uniaxial tension test of concrete, Materials and Structures 36 (2003) 365–371.
[2] Anderson, T. L., Fracture Mechanics: Fundamentals and Applications, Third Edition, CRC Press, 2004.
[3] ANSYS Users manual version 10.0, Swanson Analysis System, Inc., Houston, 2005.
[4] ASTM, Standard E 647–99: Standard Test Method for Measurement of Fatigue Crack-Growth Rates, 2000 Annual Book of ASTM Standards, Vol. 03. 01 (2000) 591–630.
[5] Bažant, Z. P., Planas, J., Fracture and size effect in concrete and other quasi-brittle materials. CRC Press, Boca Raton, 1998.
[6] Bednář, K., Two-parameter fracture mechanics: calculation of parameters and their meaning in description of fatigue cracks (in Czech), Ph.D. Thesis, IPM AS CR and BUT Brno, 1999.
[7] Brühwiler, E., Wittmann, F. H., The wedge splitting test, a new method of performing stable fracture mechanics test, Engineering Fracture Mechanics 35 (1990) 117–125.
[8] Červenka, V. et al., ATENA Program Documentation, Theory and User manual, Cervenka Consulting, Prague, 2005.
[9] Elser, M., Tschegg, E. K., Finger, N., Stanzl-Tschegg, S. E., Fracture behaviour of polypropylene-fibre reinforced concrete: an experimental investigation, Composite Science and Technology 56 (1996) 933–945.

[10] Guinea, G. V., Elices, M., Planas, J. Stress intensity factors for wedge-splitting geometry, International Journal of Fracture 81 (1996) 113–124.

[11] Hutař, P. Calculation of T-stress by means of shifted node method (in Czech), Proceedings of Problémy lomové mechaniky IV, Brno, 2004, 28–39.

[12] Hillerborg, A., Modéer, M., Petersson, P.-E., Analysis of crack formation and crack growth in concrete by means of fracture mechanics and finite elements. Cement and Concrete Research 6 (1976) 773–782.

[13] Interactive Engineering Catalogue: http://iec.skf.com.

[14] Ishiguro, S., Experiments and analyses of fracture properties of grouting mortars, Proceedings of Fracture Mechanics of Concrete and Concrete Structures – New Trends in Fracture, Catania, Taylor & Francis, 2007, 293–298.

[15] Karihaloo, B. L., Fracture mechanics and structural concrete, Longman Scientific & Technical, New York, 1995.

[16] Karihaloo, B. L., Abdalla, H., Xiao, Q. Z., Coefficients of the crack tip asymptotic field for wedge splitting specimens, Engineering Fracture Mechanics 70 (2003) 2 407–2 420.

[17] Karihaloo, B. L., Xiao, Q. Z., Higher order terms of the crack tip asymptotic field for a notched three-point bend beam. International Journal of Fracture 112 (2001) 111–128.

[18] Karihaloo, B. L., Xiao, Q. Z., Higher order terms of the crack tip asymptotic field for a wedge-splitting specimen, International Journal of Fracture 112 (2001) 129–137.

[19] Kim, J. K., Kim, Y. Y., Fatigue crack growth of high-strength concrete in wedge-splitting test, Cement and Concrete Research 29 (1999) 705–712.

[20] Knésl, Z. and Bednář, K., Two parameter fracture mechanics: calculation of parameters and their values, IPM of AS of Czech Republic, 1997.

[21] Knésl, Z., Bednář, K., Radon, J. C., Influence of T-stress on the rate of propagation of fatigue crack, Physical Mesomechanics (2000) 5–9.

[22] Larsson, S. G., and Carlsson, A. J., Influence of non-singular stress terms and specimen geometry on small scale yielding at crack tips in elastic-plastic material, Journal of Mechanics and Physics of Solids 21 (1973) 263–278.

[23] Leevers, P. S. and Radon, J. C., Inherent stress biaxiality in various fracture specimen geometries, International Journal of Fracture 19 (1983) 311–325.

[24] Linsbauer, H. N., Tschegg, E. K., Fracture energy determination of concrete with cube-shaped specimens, Zement und Beton 31 (1986) 38–40.

[25] Löfgren, I., Stang, H., Olesen, J. F., Fracture properties of FRC determined through inverse analysis of wedge splitting and three-point bending tests, Journal of Advanced Concrete Technology 3 (2005) 423–434.

[26] Murakami, Y., et al., Stress Intensity Factor Handbook I, II, III, Pergamon Press, Oxford, 1987.

[27] O'Dowd, N. P., Shih, C. F., Two-parameter fracture mechanics: theory and Applications, Fracture Mechanics, Philadelphia, 24 (1994) 21–47.

[28] Østergaard, L., Stang, H., Olesen, J. F., Time-dependent fracture of early age concrete, Proceedings of Non-Traditional Cement & Concrete, Brno, Brno University of Technology, 2002, 394–408.

[29] Pook, L. P., Linear Elastic Fracture Mechanics for Engineers: Theory and Applications, WIT Press, 2000.

[30] Rilem Report 5: Fracture Mechanics Test Methods for Concrete, Edited by S. P. Shah and A. Carpinteri and Hall, London, 1991.

[31] Seitl, S., Veselý, V., Řoutil, L., Numerical analysis of stress field for wedge splitting geometry, Proceedings of Applied Mechanics 2009, Smolenice, 2009, 270–278.

[32] Seitl, S., Dymáček, P., Klusák, J., Řoutil, L., Veselý, V., Two-parameter fracture analysis of wedge splitting test specimen, Proceedings of the 12th Int. Conf. on Civil, Structural and Environmental Engineering Computing, B. H. V. Topping, L. F. Costa Neves and R. C. Barros (eds), Funchal, Civil-Comp Press, 2009.

[33] Seitl, S., Hutař, P., Veselý, V., Keršner, Z., T-stress values during fracture in wedge splitting test geometries: a numerical study, submitted to conference Brittle Matrix Composites, Warsaw, 2009.

[34] Shah, S. P., Swartz, S. E., Ouyang, C., Fracture mechanics of structural concrete: applications of fracture mechanics to concrete, rock, and other quasi-brittle materials, John Wiley & Sons, Inc., New York, 1995.

[35] Skoček, J. and Stang, H., Inverse analysis of the wedge-splitting test, Engineering Fracture Mechanics 75 (2008) 3 173–3 188.

[36] Tada, H., Paris, P. C., Irwin, G. R., The Stress Analysis of Cracks Handbook, Third Edition, ASME, New York, 2000.

[37] Tan, C. L., Wang, X., The use of quarter-point crack-tip elements for T-stress determination in boundary element method analysis, Engineering Fracture Mechanics 70 (2003) 2 247–2 252.

[38] Trunk, B., Schober, G., Wittmann, F. H., Fracture mechanics parameters of autoclaved aerated concrete. Cement and Concrete Research 29 (1999) 855–859.

[39] van Mier, J. G. M., Fracture processes of concrete: Assessment of material parameters for fracture models, CRC Press, Boca Raton, 1997.

[40] van Vliet, M. R., van Mier, J. G. M., Experimental investigation of size effect in concrete and sandstone under uniaxial pension, Engineering Fracture Mechanics 65 (2000) 165–188.

[41] Veselý, V., Parameters of concrete for description of fracture behaviour (in Czech). Ph.D. thesis, Brno University of Technology, Faculty of Civil Engineering, Brno, Czech Republic, 2004.

[42] Veselý, V., Frantík, P., Development of fracture process zone in quasi-brittle bodies during failure, Proceedings of Engineering Mechanics 2009, Svratka, 288–289 + 12 p. (CD – in Czech).

[43] Veselý, V., Frantík, P., Keršner, Z., Cracked volume specified work of fracture, Proceedings of the 12th Int. Conf. on Civil, Structural and Environmental Engineering Computing, B. H. V. Topping, L. F. Costa Neves and R. C. Barros (eds), Funchal, Civil-Comp Press, 2009.

[44] Vořechovský, M., Sadílek, V., Computational modeling of size effects in concrete specimens under uniaxial tension. International Journal of Fracture 154 (2009) 27–49.

[45] Williams, M. L., On the stress distribution at the base of stationary crack, ASME Journal of Applied Mechanics 24 (1957) 109–114.

[46] Xiao, J., Schneider, H., Donnecke, C., Konig, G., Wedge splitting test on fracture behaviour of ultra high strength concrete, Construction and Building Materials 18 (2004) 359–365.

[47] Xu, S., Bu, D., Gao, H., Yin, S., Liu, Y., Direct measurement of double-K fracture parameters and fracture energy using wedge-splitting test on compact tension specimens with different size, Proceedings of Fracture Mechanics of Concrete and Concrete Structures – New Trends in Fracture, Catania, Taylor & Francis, 2007, 271–278.

[48] Wang, J. M., Zhang, X. F., Xu, S. L., The experimental determination of double-K fracture parameters of concrete under water pressure, Proceedings of Fracture Mechanics of Concrete and Concrete Structures – New Trends in Fracture, Catania, Taylor & Francis, 2007, 279–284.

[49] Yang, B., Ravi-Chandar, K., Evaluation of elastic T-stress by the stress difference method, Engineering Fracture Mechanics 64 (1999) 589–605.